

Table of content

Appendix Figure S1. VE-PTP polarization and deletion in VE-PTP^{iECKO} mice or by siRNA.

Appendix Figure S2. Flow-induced downstream polarization of VE-PTP in HUVEC.

Appendix Figure S3. VEGFR2 and RhoA are not essential for shear stress-mediated redistribution of VE-PTP.

Appendix Figure S4. Validation of method for leakage measurement.

Appendix Figure S5. Specificity of Tie2-pY992 antibodies.

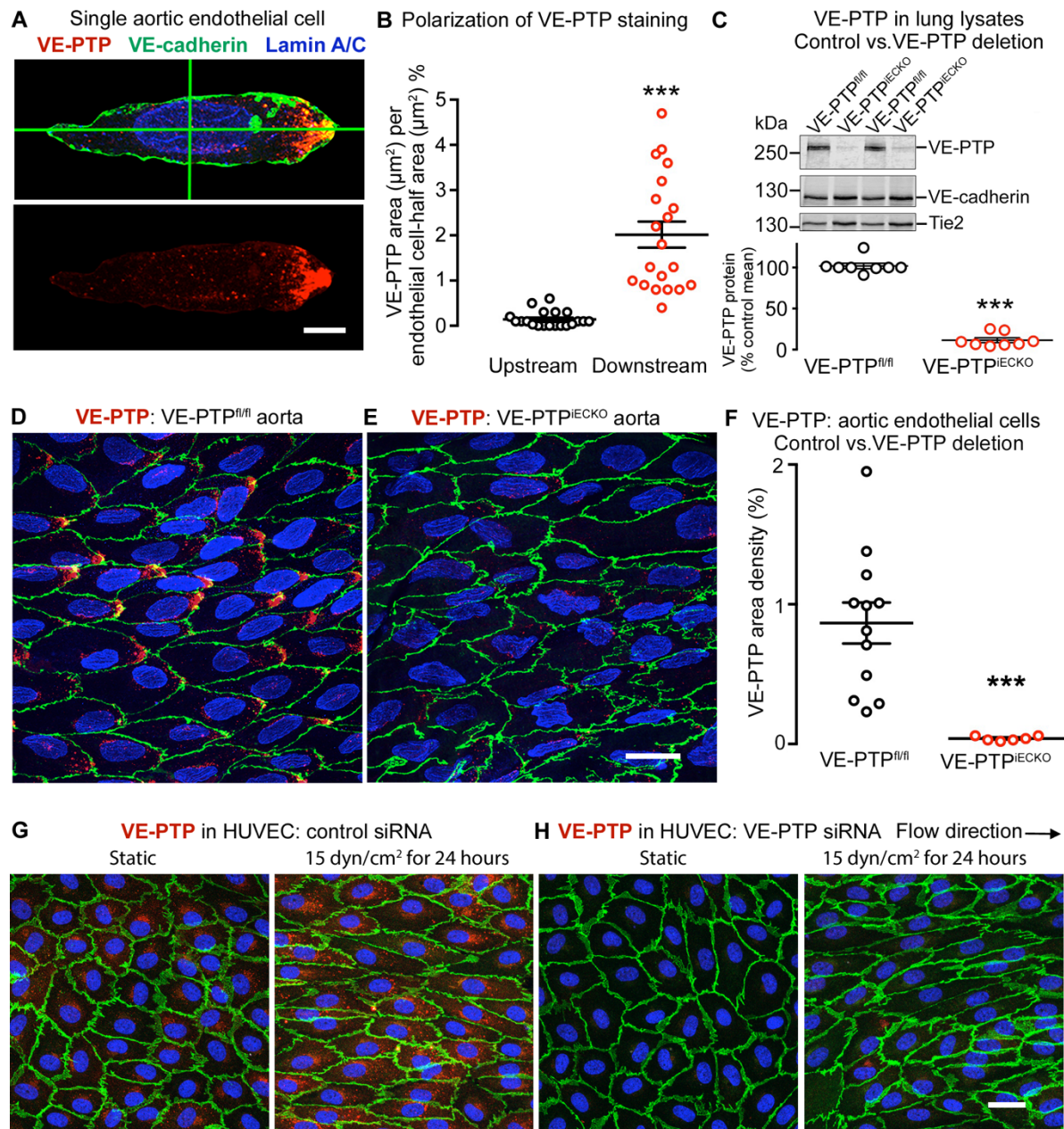
Appendix Figure S6. VE-PTP deletion in ApoE^{-/-} mice without changes in body weight and plasma lipids.

Appendix Figure S7. Oil Red O staining of atheromas in the aortic root.

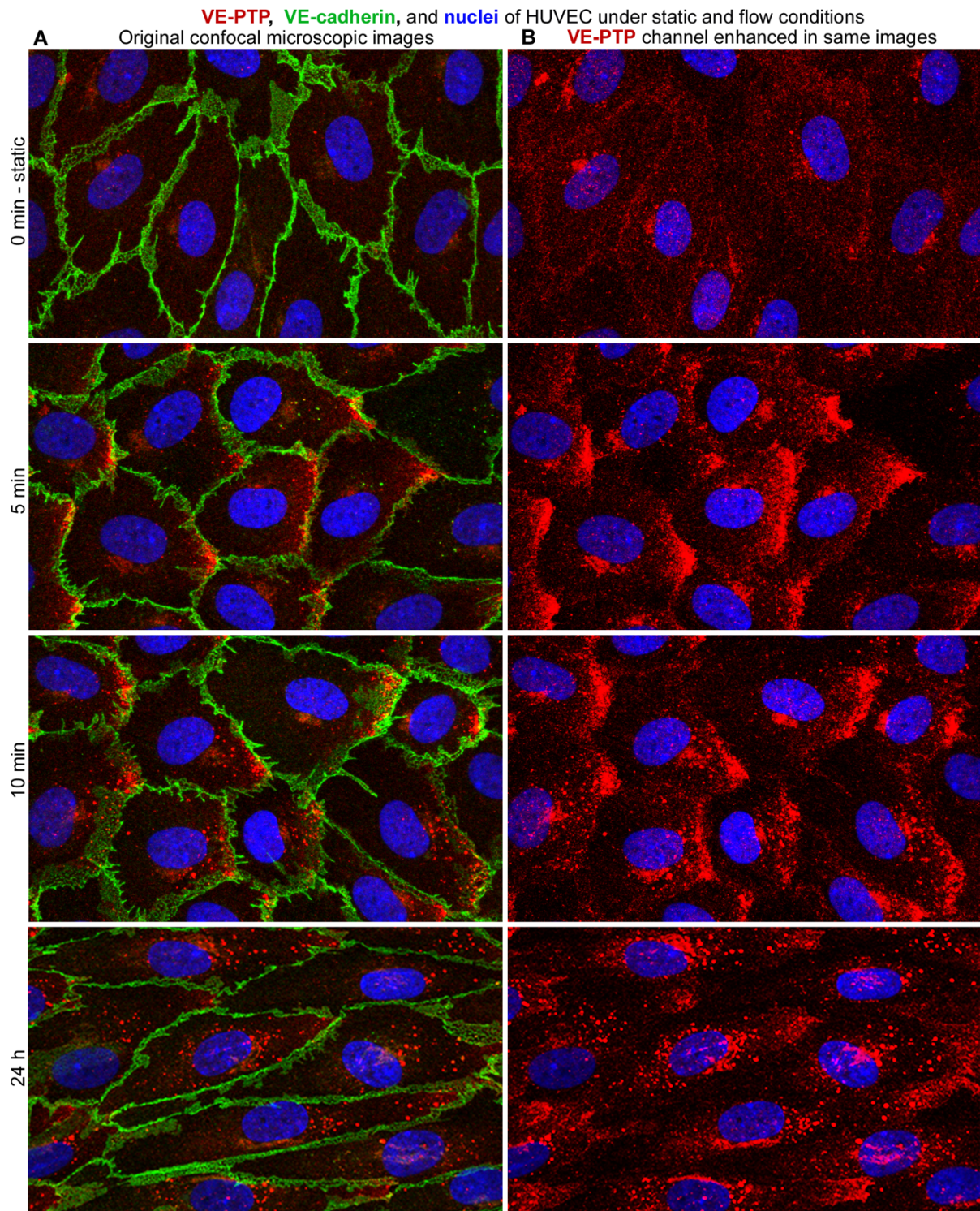
Appendix Figure S8. Contrasting staining of Tie2-pY992 and VE-cadherin at endothelial cells of normal region and over atheroma.

Appendix Figure S9. VE-PTP inhibitor AKB-9785 increases Tie2-pY992 at both cellular junctions and focal adhesions.

Appendix Figure S10. Increased Tie2 phosphorylation after AKB-9785 without changes in body weight or plasma lipids.

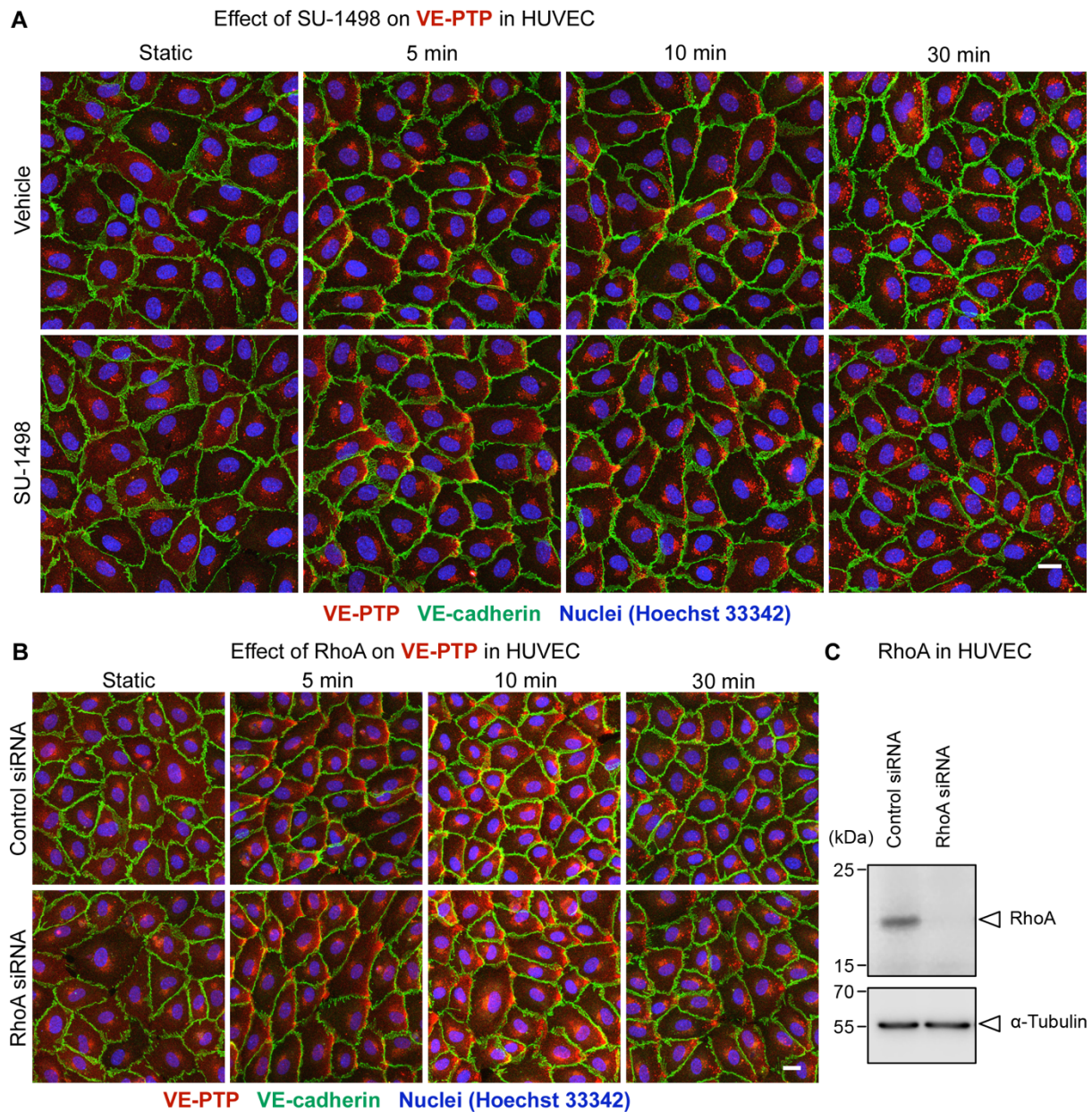


Appendix Figure S1. VE-PTP polarization and deletion in VE-PTP^{IECKO} mice or by siRNA. (A-B) Images and measurements documenting VE-PTP polarization (red) in individual endothelial cells in thoracic aorta of wild-type mouse. Values in B compare the amounts of VE-PTP staining in each cell half. Each dot represents half of one endothelial cell. Mean \pm SEM, $n = 15$ cells. (C) Assessment of VE-PTP deletion (89%) by immunoblot of lung lysates. VE-PTP protein expressed as a ratio to VE-cadherin protein. Mean \pm SEM, $n = 8$ mice/group. (D-E) Comparison of VE-PTP staining (red) of endothelial cells in thoracic aorta of VE-PTP^{fl/fl} mouse and VE-PTP^{IECKO} mouse. (F) Assessment of VE-PTP deletion (95%) in E by immunohistochemical staining. Mean \pm SEM, $n = 6-12$ mice/group. (G-H) Comparison of staining for VE-PTP (red), VE-cadherin (green), and nuclei (blue, Hoechst 33342) in HUVEC after control siRNA in G or VE-PTP siRNA in H under static conditions or laminar flow of 15 dyn/cm² for 24 h. *** $P < 0.001$, by Student's t -test in B and F and Mann-Whitney-test in C. Scale bars: 10 μ m in A, 20 μ m in D, E, G and H.

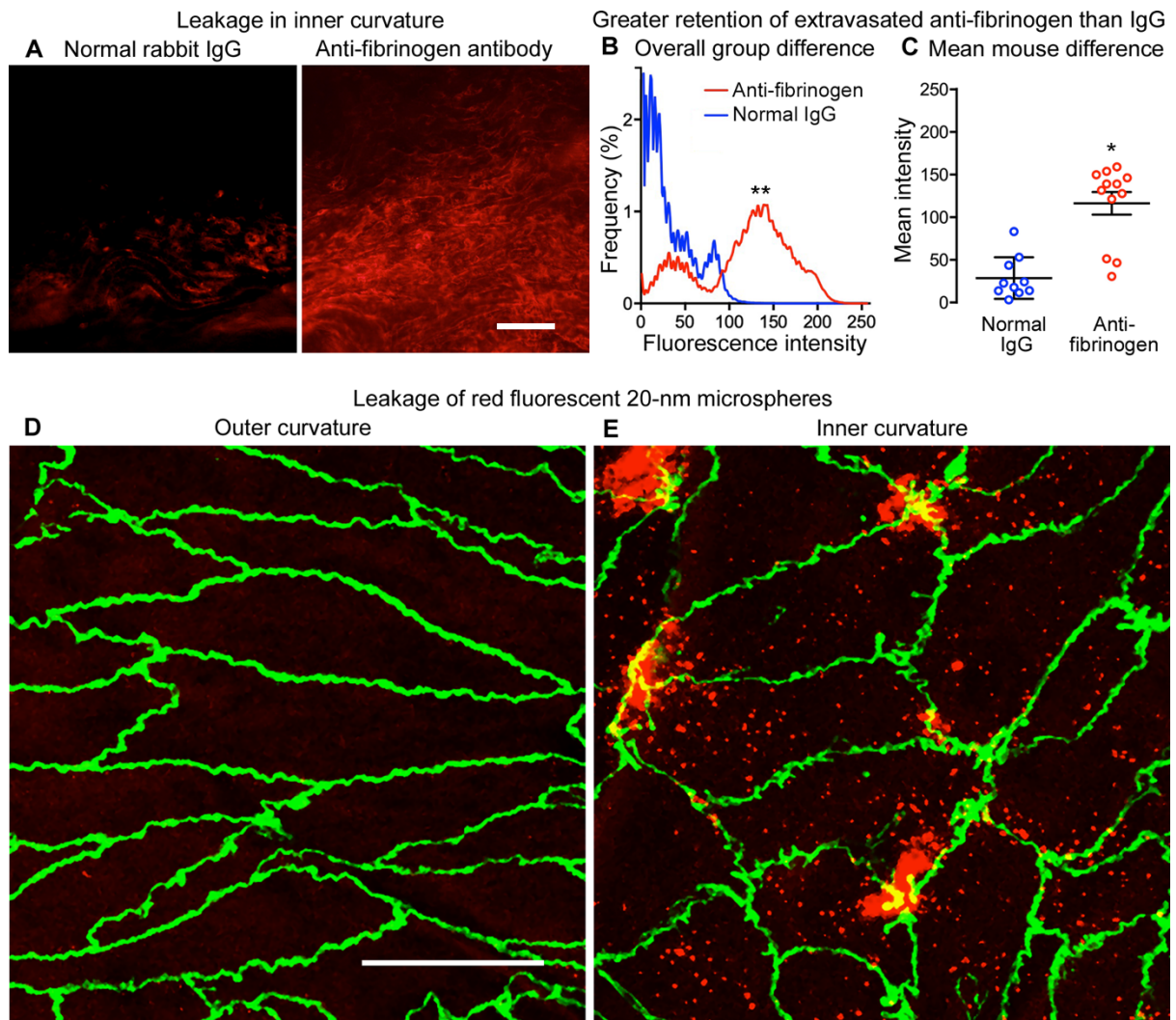


Appendix Figure S2. Flow-induced downstream polarization of VE-PTP in HUVEC. (A-B) Enlargements of images in Figure 1G showing VE-PTP staining (red) in HUVEC under static conditions and laminar flow (15 dyn/cm²) for 5 min to 24 h to compare the original confocal microscopic images in A to the same images in B after the brightness and contrast of red channel (VE-PTP) were increased to highlight the flow-induced changes. VE-cadherin, green. Nuclei, blue (Hoechst 33342). All images in B were treated identically. Faint VE-PTP staining at the cell border and near the nucleus under static conditions contrasts with downstream polarization after flow and change from diffuse downstream staining at 5 min to

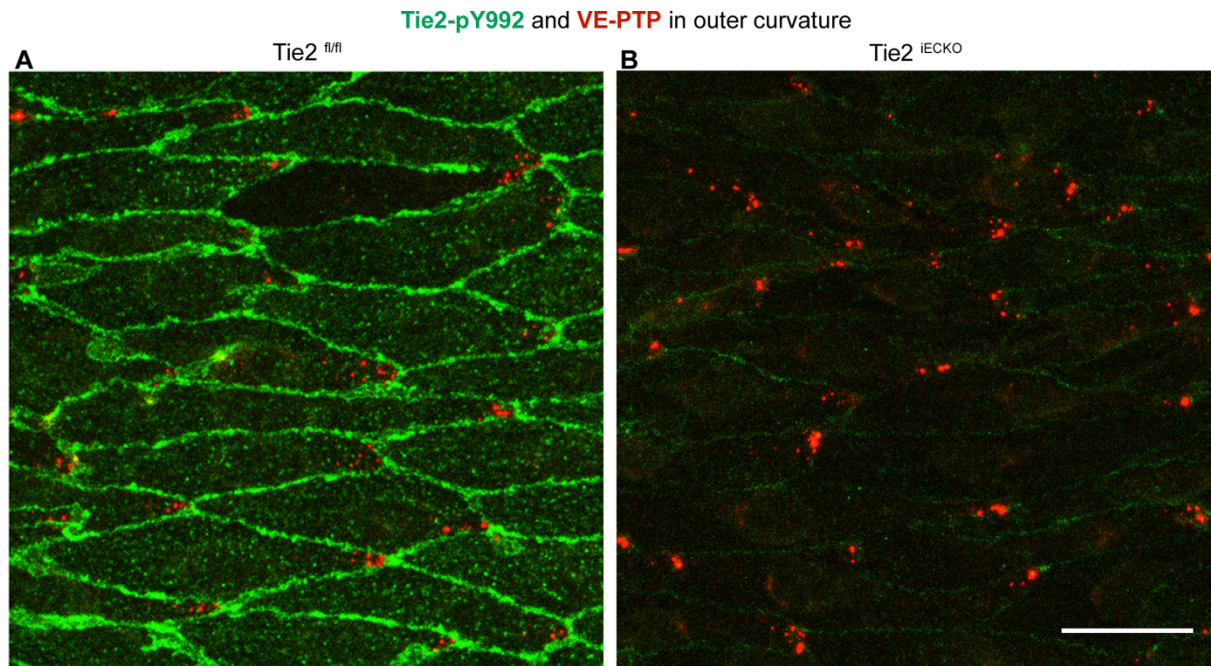
dot-like downstream staining at 10 min, and more widespread dot-like staining at 24 h.
Scale bar: 10 μm .



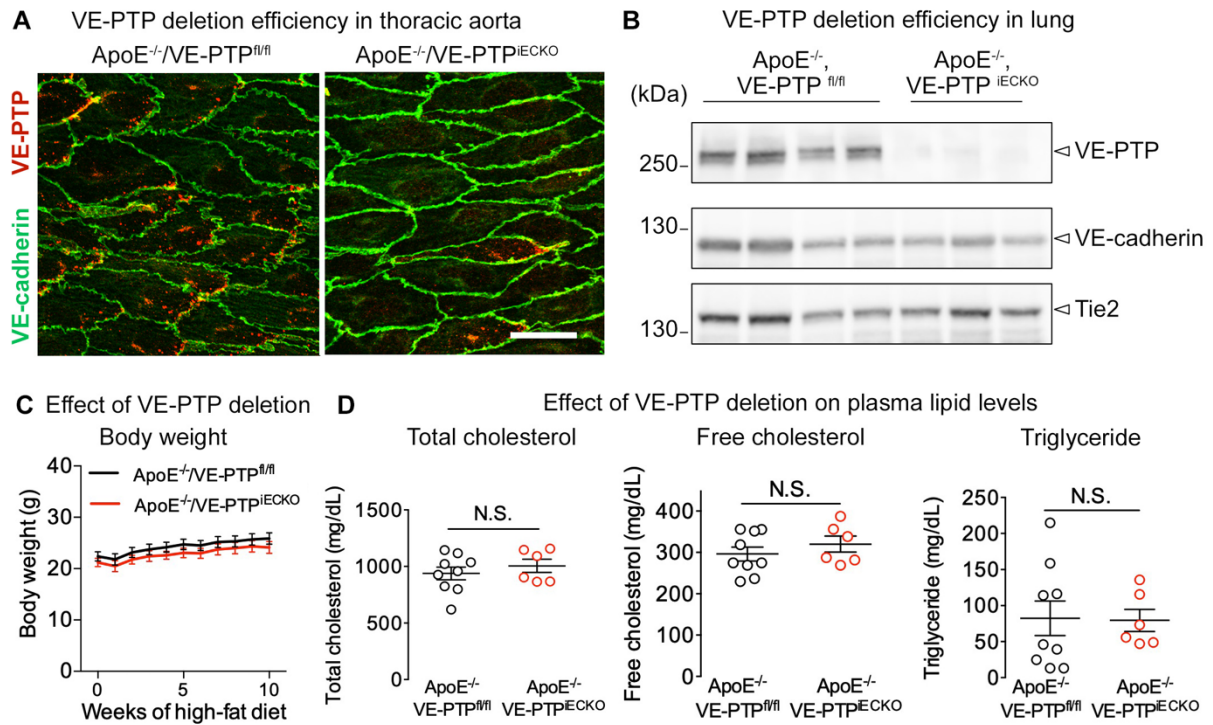
Appendix Figure S3. VEGFR2 and RhoA are not essential for shear stress-mediated redistribution of VE-PTP. (A) HUVECs, treated with DMSO or SU-1498 for four hours, were exposed to 15 dyn/cm² of shear stress for indicated times. The resulting cells were fixed and stained for VE-PTP (red) and VE-cadherin (green) and Hoechst 33342 (blue). (B) HUVECs treated with control siRNA or RhoA siRNA were exposed to shear and stained similarly as under A. (C) Cell lysates of HUVEC treated with control siRNA or RhoA siRNA were immunoblotted for RhoA and tubulin, as indicated. Molecular weights are given on the left. Scale bar: 20 μ m.



Appendix Figure S4. Validation of method for leakage measurement. (A) Fluorescence microscopic images comparing intensity of extravasated normal rabbit IgG or anti-fibrinogen antibody in inner curvature of aortic arch of wild-type mice. (B) Comparison of distribution of fluorescence intensities of normal rabbit IgG and anti-fibrinogen antibody in inner curvature. (C) Mean fluorescence intensity in each mouse for data in B. Mean \pm SEM, $n = 10-12$ mice/group. (D-E) Confocal microscopic images comparing little extravasation of 20-nm red fluorescent microspheres in the outer curvature in D to focal sites of leakage in the inner curvature in E of the same wild-type mouse. The brightest patches of microspheres are near endothelial cell junctions. VE-cadherin (green). * $P < 0.05$, ** $P < 0.01$, by Kolmogorov-Smirnov two-sample test in B and Student's t -test in C. Scale bars: 100 μm in A, 20 μm in D and E.

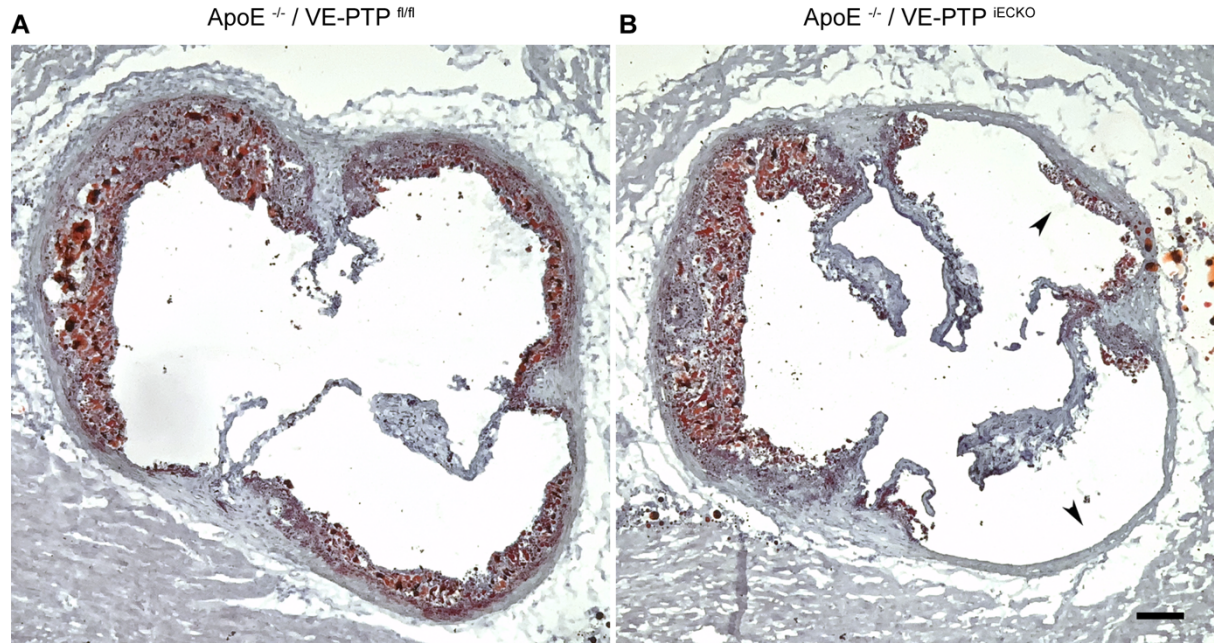


Appendix Figure S5. Specificity of Tie2-pY992 antibodies. (A-B) Comparison of staining for pY992-Tie2 of aortic endothelial cells in the outer curvature of Tie2^{fl/fl} and Tie2^{iECKO} mice, as indicated. Scale bar: 20 μ m.

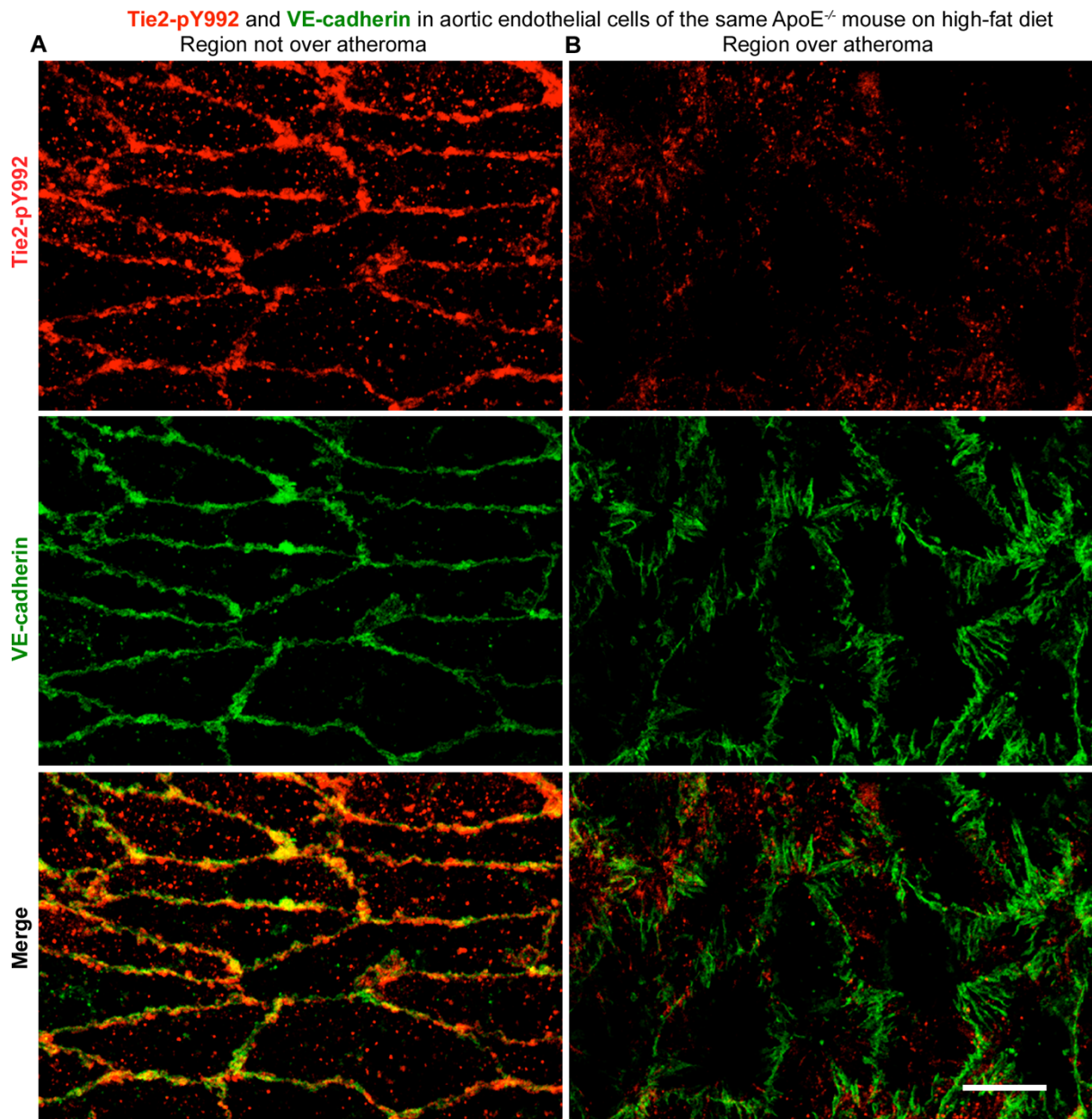


Appendix Figure S6. VE-PTP deletion in ApoE^{-/-} mice without changes in body weight and plasma lipids. **(A)** Contrasting amounts of VE-PTP (red) staining in thoracic aorta of control ApoE^{-/-}/VE-PTP^{fl/fl} mouse and ApoE^{-/-}/VE-PTP^{iECKO} mouse, in which VE-PTP was deleted in endothelial cells. VE-cadherin (green). **(B)** Confirmation of VE-PTP deletion by VE-PTP protein in lung lysates of control ApoE^{-/-}/VE-PTP^{fl/fl} mice and ApoE^{-/-}/VE-PTP^{iECKO} mice. **(C-D)** No significant difference in body weight of ApoE^{-/-}/VE-PTP^{fl/fl} mice (n = 18 mice) and ApoE^{-/-}/VE-PTP^{iECKO} mice (n = 13 mice) in C or in plasma lipids in ApoE^{-/-}/VE-PTP^{fl/fl} mice (n = 9 mice) and ApoE^{-/-}/VE-PTP^{iECKO} mice (n = 6 mice) in D. Mean ± SEM. N.S. not significant, by Welch's *t*-test in D. Scale bar: 20 μm.

Oil Red O-stained atheromas in aortic root

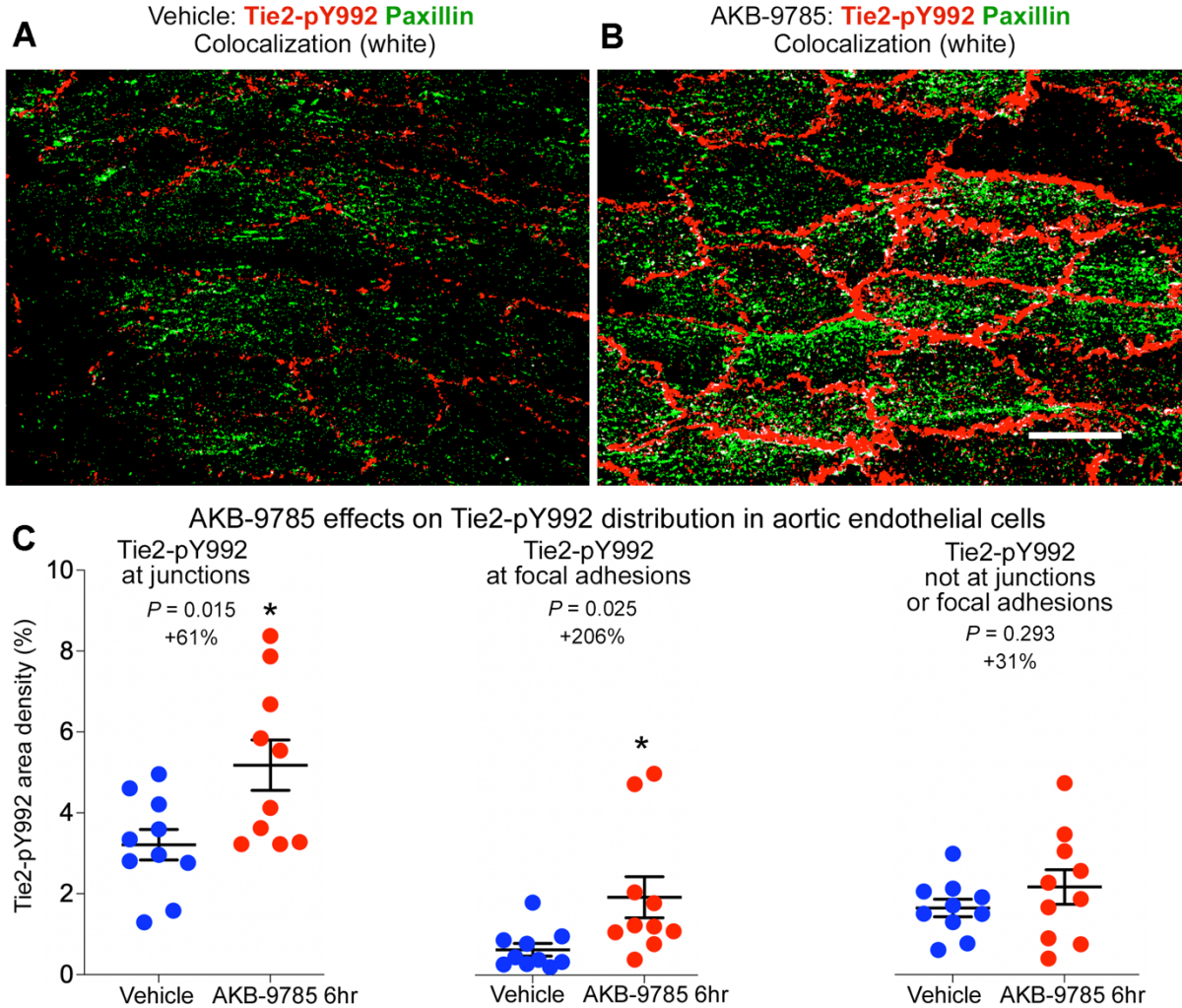


Appendix Figure S7. Oil Red O staining of atheromas in the aortic root. (A) ApoE^{-/-}/VE-PTP^{fl/fl} mice and (B) ApoE^{-/-}/VE-PTP^{iECKO} mice were fed for 10 weeks with a high fat diet followed by preparing 8 μ m cryostat sections of the aortic root in the plane of the aortic valve and staining with Oil Red O. Scale bar 100 μ m.

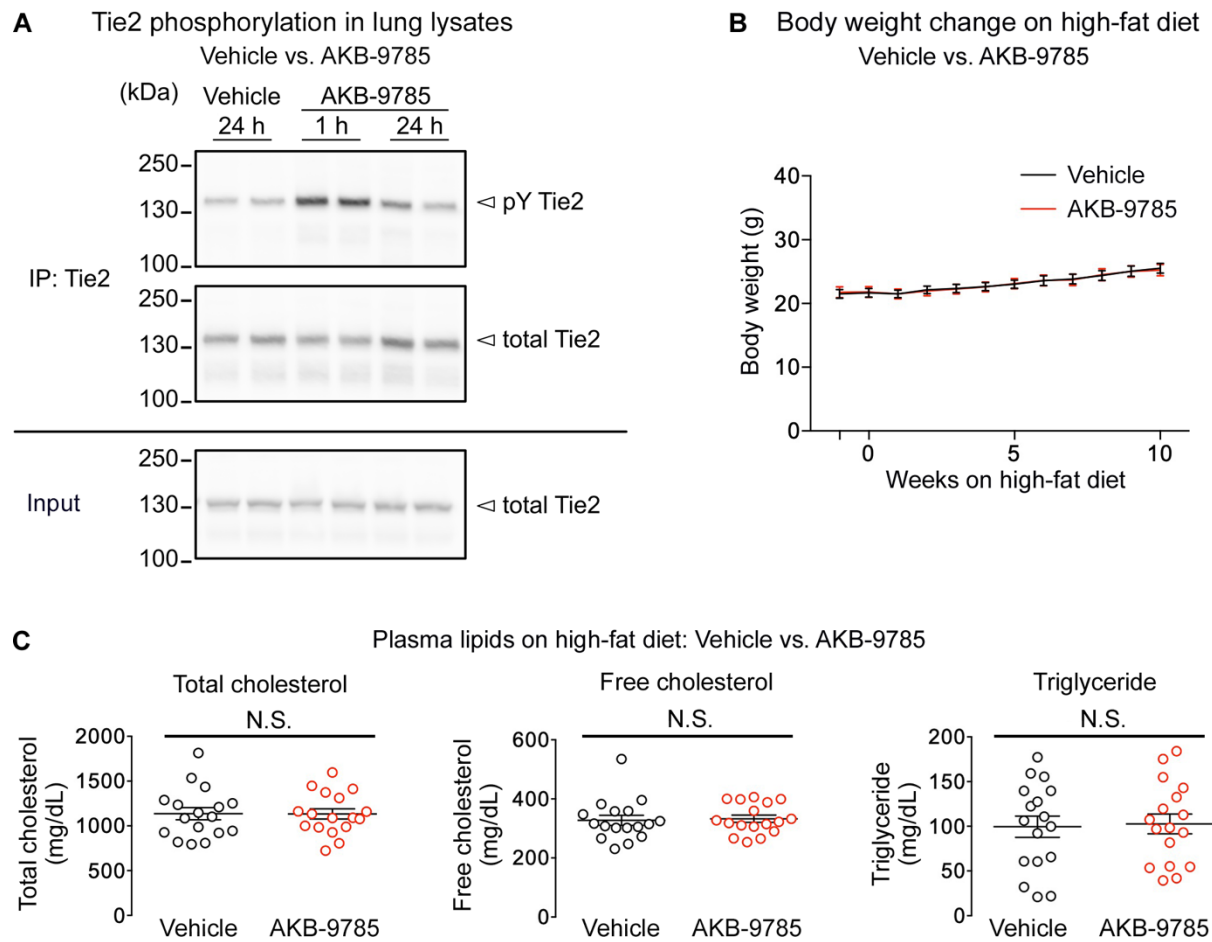


Appendix Figure S8. Contrasting staining of Tie2-pY992 and VE-cadherin at endothelial cells of normal region and over atheroma. (A-B) Strong staining for Tie2-pY992 in endothelial cells of a normal region of aortic arch in A compared to weak staining in endothelial cells over an atheroma in B in the aortic arch of the same ApoE^{-/-} mouse on high-fat diet. VE-cadherin is also strikingly different, where staining delineates roughly linear cell borders in the normal region in A but has a zig-zag pattern in B that reflects the complex jagged contour of endothelial cell borders over the atheroma. Scale bar: 10 μ m.

AKB-9785 (2 doses over 6 hr) effects on Tie2-pY992 in endothelial cells of thoracic aorta



Appendix Figure S9. VE-PTP inhibitor AKB-9785 increases Tie2-pY992 at both cellular junctions and focal adhesions. (A) Mice were treated subcutaneously twice with vehicle or (B) with AKB-9785 over a period of 6 h, followed by staining of the thoracic aorta endothelium by antibodies against Tie2-pY992 (red) and paxillin (green). (C) Tie2-pY992 staining area density was quantified at endothelial junctions (left), at paxillin stained focal adhesions (middle) and at sites outside these areas (right), for vehicle treated (blue) and AKB-9785 treated (red) mice. Mean \pm SEM, n = 10 /group, *P < 0.05 by unpaired Student's t-test in C



Appendix Figure S10. Increased Tie2 phosphorylation after AKB-9785 without changes in body weight or plasma lipids. (A) Phosphorylation of Tie2 in lung lysates of wild-type mice at 1 and 24 h after a single subcutaneous dose of vehicle or AKB-9785 (30 mg/kg, 100 μ L of 10 mM to 20 g mice) showing a peak at 1 h after AKB-9785. Immunoprecipitates (IP) or lung lysates were immunoblotted for phosphotyrosine (antibody 4G10) or total Tie2. (B) Similar body weight of ApoE^{-/-} mice on high-fat diet after daily treatment with vehicle or AKB-9785. (C) Absence of difference in plasma lipids in ApoE^{-/-} mice after treatment with vehicle or AKB-9785. Mean \pm SEM, n = 17 mice/group, N.S. not significant, by Welch's *t*-test in C.